Published in final edited form as:

Colloids Surf B Biointerfaces. 2017 October 01; 158: 356–362. doi:10.1016/j.colsurfb.2017.07.014.

Contribution of Kupffer cells to liposome accumulation in the liver

Emma Samuelsson[a], **Haifa Shen**[a,b], **Elvin Blanco**[a], **Mauro Ferrari**[a,c,*], and **Joy Wolfram**[a,d,*]

[a]Department of Nanomedicine, Houston Methodist Research Institute, Houston, TX 77030, USA

[b]Department of Cell and Developmental Biology, Weill Cornell Medicine, New York, NY 10065, USA

[c]Department of Medicine, Weill Cornell Medicine, Weill Cornell Medicine, New York, NY 10065, USA

[d]Department of Transplantation, Mayo Clinic, Jacksonville, Florida 32224, USA

Abstract

The liver is a major barrier for site-specific delivery of systemically injected nanoparticles, as up to 90% of the dose is usually captured by this organ. Kupffer cells are thought to be the main cellular component responsible for nanoparticle accumulation in the liver. These resident macrophages form part of the mononuclear phagocyte system, which recognizes and engulfs foreign bodies in the circulatory system. In this study, we have compared two strategies for reducing nanoparticle accumulation in the liver, in order to investigate the specific contribution of Kupffer cells. Specifically, we have performed a comparison of the capability of pegylation and Kupffer cell depletion to reduce liposome accumulation in the liver. Pegylation reduces nanoparticle interactions with all types of cells and can serve as a control for elucidating the role of specific cell populations in liver accumulation. The results indicate that liposome pegylation is a more effective strategy for avoiding liver uptake compared to depletion of Kupffer cells, suggesting that nanoparticle interactions with other cells in the liver may also play a contributing role. This study highlights the need for a more complete understanding of factors that mediate nanoparticle accumulation in the liver and for the exploration of microenvironmental modulation strategies for reducing nanoparticle-cell interactions in this organ.

Keywords

Kupffer cells; liver; macrophages; mononuclear phagocyte system; nanoparticles; pegylation

[*]Corresponding authors. Tel.: +1 (713) 441-8439 (M.F.), +1 (713) 441-8939 (J.W); fax: +1 (713) 441-3655. mferrari@houstonmethodist.org (M.F), jvwolfram@houstonmethodist.org (J.W).

Conflict of interest

The authors declare no conflicts of interest.

1. Introduction

Patient survival and quality of life are highly dependent on biodistribution of administered drugs. For many diseases, including metastatic cancer, it is challenging or impossible to locally administer therapeutic agents, necessitating the use of the circulatory system for drug delivery. Strategies that increase the accumulation of systemically administered drugs in diseased tissues improve therapeutic efficacy and minimize side effects. For instance, nanocarriers can enhance localized delivery of therapeutic agents by incorporating transport enhancing components, such as targeting ligands and sustained/triggered-release systems, and by taking advantage of transport phenomena that appear on the nanoscale, e.g. reduced renal clearance and the enhanced permeability and retention effect [1, 2]. Studies have demonstrated that nanodelivery can substantially increase the tumor accumulation of small molecules [3, 4]. However, in most cases, less than 1% of the intravenously injected nanoparticle dose reaches the intended location [5] and up to 90% accumulates in the liver [6]. Despite the fact that the liver is a major barrier for drug delivery, mechanisms for nanoparticle accumulation in this organ are poorly understood. In particular, it is unclear to what extent each component of the liver contributes to nanoparticle deposition, and it is thought that both cells and physical features play a role [7]. Specifically, the physical organization of the vascular network in the liver is likely to be a major contributing factor [8, 9]. In regards to cellular components, Kupffer cells, which are the resident macrophages of the liver, are considered to be largely responsible for cellular uptake of nanoparticles in this organ [6]. These phagocytes engulf damaged cells and foreign material, such as bacteria, viruses, and nanoparticles [10], and make up 80–90% of the total macrophage population in the body [11]. In the circulatory system, nanoparticles interact with plasma proteins, which form a protein corona around the particle surface [12]. Opsonins such as immunoglobulins and complement proteins trigger phagocytosis by binding to membrane receptors on Kupffer cells [12]. The most widely used strategy for reducing nanoparticle interactions with macrophages is to coat the particle surface with polyethylene glycol (PEG) [13]. PEG attracts water molecules that form a hydration layer, which reduces protein binding and cell interactions. Notably, the stealth effect is not specific to macrophages, since this hydration layer reduces interactions with all types of cells [14, 15].

In this study, we compared two different strategies for decreasing nanoparticle accumulation in the liver (Fig. 1). The first strategy entailed pegylation of nanoparticles, while the second strategy involved Kupffer cell depletion prior to nanoparticle administration. The nanoparticles used in this study were liposomes as they represent one of the largest categories of clinically approved nanodrugs. There are currently over a dozen liposomal drug formulations on the market used for treatment of various conditions, including fungal infections and cancer [16, 17]. The objective of this study was to investigate the specific contribution of Kupffer cells to cell-mediated accumulation of liposomes in the liver. This goal was achieved by using pegylation as a control for examining the role of Kupffer cells in nanoparticle uptake, since PEG reduces interactions with all cell types.

2. Materials and methods

2.1. Materials

Materials were acquired from the following sources: dioleoyl-phosphatidylcholine (DOPC)/cholesterol (CHOL) liposomes (F60103F-TR) and DOPC/CHOL/mPEG-distearoyl-phosphoethanolamine (DSPE) liposomes (F60203F-TR) labeled with Texas Red-dihexadecanoyl-phosphoethanolamine from FormuMax Scientific; clodronate liposomes from Encapsula NanoSciences; Prigrow II Medium and immortalized rat Kupffer cells from Applied Biological Materials; Raw 264.7 mouse macrophage cells from American Type Culture Collection (ATCC); fetal bovine serum (FBS) from Atlas Biologicals; 96-well flat clear bottom black polystyrene TC-treated microplates and Dulbecco's Modified Eagle's Medium (DMEM) with 4.5 g/L glucose, L-glutamine & sodium pyruvate from Corning; penicillin-streptomycin solution from Sigma-Aldrich; ethylendiaminetetraacetic acid (EDTA) and phosphate buffered saline (PBS; HyClone) from Thermo Fisher Scientific; F4/80: Alexa Fluor 647 antibody from Bio-Rad (MCA497A488); CellTiter 96 AQueous Non-Radioactive Cell Proliferation Assay from Promega; Microtainer Tubes with K2E from BD; Amicon Ultra-15 Centrifugal Filter Device 100K from Millipore Sigma; Tissue-Tek optimum cutting temperature (O.C.T) compound form VWR; Vectashield Antifade Mounting Medium with DAPI (4′,6-diamidino-2-phenylindole) and normal horse serum from Vector Laboratories.

2.2. Nanoparticle characterization and stability

Dynamic light scattering and laser Doppler micro-electrophoresis were used to measure the size and zeta potential of liposomes (0.5% v/v in distilled water), respectively, using a Zetasizer Nano ZS (ZEN 3600, Malvern Instruments) as previously reported [18–20]. The fluorescence intensity (Ex/Em of 590 nm/620 nm) of serial dilutions of the liposome stock solution was measured in black clear-bottom 96-well microplates with a Synergy H4 Hybrid Microplate Reader (BioTek). Dynamic light scattering was used to measure liposomal stability at various time points under physiological conditions. Liposomes were incubated in Prigrow II Medium with 10% FBS (2.7% v/v) on a shaker at 37°C and the size was measured in distilled water (2% v/v) as described above. The detachment of fluorophore from liposomes was also measured at 37°C on a shaker (0.2% v/v in Prigrow II Medium with 10% FBS). At various time points, centrifugation (4000 × g; 30 min) of the media solution was performed in Amicon Ultra-15 Centrifugal Filter Device 100K. The fluorescence intensity of the ultrafiltrate was measured as described above

2.3. Liposome uptake and cell viability *in vitro*

Kupffer cells and Raw 264.7 cells were cultured in PriGrow II Media and DMEM, respectively. The media was supplemented with 1% penicillin (10,000 units/mL)-streptomycin (10 mg/mL) solution and 10% FBS and cells were incubated at 37°C and 5% CO_2. Experiments were performed with cells grown in culture for less than ten passages. Cells were grown to 80% confluency in 96-well plates and incubated with fluorescent non-pegylated and pegylated liposomes (200 μM of lipids) for 3 h. Cells were washed three times in PBS and liposome uptake in live cells was visualized with an Eclipse Ti Inverted Fluorescence Microscope (Nikon). Quantitative measurements of fluorescence intensity

(Ex/Em of 590 nm/620 nm) were performed on a H4 Hybrid Microplate Reader (BioTek). The background fluorescence from untreated cells was subtracted from the obtained values. Cell viability measurements were then performed with a CellTiter 96 AQueous Non-Radioactive Cell Proliferation Assay according to the manufacturer's instructions.

2.4. Liposome biodistribution

Animal studies were conducted in accordance with the guidelines of the Animal Welfare Act and the National Institutes of Health Guide for the Care and Use of Laboratory Animals following a protocol approved by the Institutional Animal Care and Use Committee at the Houston Methodist Research Institute. Athymic nude mice purchased from Charles River (female; 6–8 weeks; ~22 g) were intravenously injected with PBS (control mice) or clodronate liposomes (clodrolip; 50 mg/kg clodronate) [21]. Mice were intravenously administered with fluorescent pegylated or non-pegylated liposomes (100 μL/mouse; 50 mM lipids). The liver, spleen, and plasma were collected 24 h post-injection. Blood collection was performed through cardiac puncture with needles pre-rinsed in EDTA (0.5 M; pH 8) and plasma was obtained through centrifugation in Microtainer Tubes with K2E (10 min; 3000 × g). A T25 Digital Ultra Turrax Homogenizer (Ika) was used to homogenize preweighed organs (1 g tissue/3 mL PBS). The fluorescence intensity (Ex/Em of 590 nm/620 nm) of serial dilutions of the samples was measured in black clear-bottom 96-well plates with a Synergy H4 Hybrid Microplate Reader (BioTek). Homogenized organs and plasma samples from untreated mice served as a background signal that was subtracted from the liposome samples.

2.5. Immunofluorescence staining

Mice were sacrificed 24 h post-injection of PBS (control mice) or clodrolip (50 mg/kg clodronate). Livers were placed in Tissue-Tek optimum cutting temperature (O.C.T) compound on dry ice. Immunofluorescence staining was performed on frozen acetone fixed liver sections (6 μm). The slides were blocked in 2.5% normal horse serum, incubated with a F4/80-Alexa Fluor 647 antibody (1:10 dilution) overnight at 4°C, and mounted with Vectashield Antifade Mounting Medium with DAPI. The slides were visualized using a Nikon A1 Confocal Imaging System.

3. Results and discussion

3.1. Liposome characteristics and stability

Prior to assessing nanoparticle uptake *in vitro* and biodistribution *in vivo*, the size, polydispersity index (PDI), zeta potential, and fluorescence intensity of the liposomes was measured. Dynamic light scattering revealed that the non-pegylated and pegylated liposomes had a size of 111.7 ± 4.2 nm and 99.4 ± 1 nm, respectively (Fig. 2a), which is similar to the size of liposome formulations on the market [22, 23]. Moreover, the DOPC/cholesterol (54:45 molar ratio) liposome composition used in this study closely resembles the phospholipid/cholesterol content of the clinically approved liposomes Doxil (55:40 molar ratio) and Myocet (55:45 molar ratio) [23]. The PDI of the non-pegylated and pegylated liposomes was less than 0.3 (Fig. 2b), indicating that the liposomes had a relatively homogeneous size distribution. Laser Doppler micro-electrophoresis demonstrated that the

zeta potential of the pegylated liposomes (−62.8 ± 0.3 mV) was substantially lower than that of the non-pegylated liposomes (−15.6 ± 0.6 mV) (Fig. 2c). These results are in accordance with a previous report that showed that PEG lowers the zeta potential of liposomes [24]. Fluorescence measurements revealed that the non-pegylated and pegylated liposomes had the same fluorescence intensity (Fig. 2d), which is critical for comparison studies of liposome biodistribution and uptake in cells. The stability of the liposomes under physiological conditions was also evaluated. After a 24 h incubation period, the size (Fig. 3a) and PDI (Fig. 3b) of the liposomes remained unchanged, indicating that the nanoparticles were stable. Moreover, the detachment of fluorophore from the liposomal membrane was assessed to ensure that the majority of the detected fluorescence signal originated from the liposomes. The results indicate that after 24 h under physiological conditions, only 0.4% (non-pegylated liposomes) and 0.3% (pegylated liposomes) of the fluorescence signal had detached from the liposomal membrane (Fig. 3c).

3.2. Liposome uptake by macrophages

The uptake of non-pegylated and pegylated liposomes was assessed in Kupffer cells and Raw 264.7 cells. As expected, fluorescence microscopy revealed that the uptake of non-pegylated liposomes was substantially higher than that of pegylated liposomes (Fig. 4a). Moreover, quantitative measurements of fluorescence intensity demonstrated that the uptake of non-pegylated liposomes was 4.6-fold and 23.9-fold higher than pegylated liposomes in Raw 264.7 cells (Fig. 4b) and Kupffer cells (Fig. 4d), respectively. Cell viability assays were performed to confirm that the viability of Raw 264.7 cells (Fig. 4c) and Kupffer cells (Fig. 4e) remained unchanged in response to liposome exposure.

3.3. Liposome accumulation in the plasma, liver, and spleen

The accumulation of intravenously injected fluorescent non-pegylated and pegylated liposomes in the plasma, liver, and spleen was assessed by measuring the fluorescence intensity of homogenized organs. As expected, the pegylated liposomes had a higher plasma concentration than non-pegylated liposomes after 24 h (Fig. 5). Moreover, liposomal pegylation led to a 64.4% reduction in liver accumulation (Fig. 5). Likewise, spleen accumulation of pegylated liposomes was substantially reduced compared to that of non-pegylated liposomes (Fig. 5). The well-known macrophage depletion agent clodrolip [21] was used to completely deplete Kupffer cells in the liver. The clodrolip dose used in these studies has previously been shown to primarily deplete macrophages in the liver [25]. Immunofluorescence staining of liver sections was performed to confirm clodrolip-induced depletion of Kupffer cells (Fig. 6a). For the first time, a side-by-side comparison of the effects of pegylation and Kupffer cell depletion on liposome accumulation in the liver was performed to evaluate the role of macrophages in organotropic deposition. Liposomal pegyaltion caused the plasma/liver accumulation ratio to increase from 0.1 to 11.6, while the corresponding value was 2.9 in the Kupffer cell depletion group (Fig. 6b). These results suggest that Kupffer cells may not the only cells responsible for liposome deposition in the liver, as pegylation can be used as a control for reducing interactions with all types of cells. In the case that Kupffer cells had been solely responsible for cell-mediated uptake of liposomes in the liver, the macrophage depletion strategy would have been equally or more effective than pegylation, as PEG may not inhibit all cell interactions. The plasma/spleen

accumulation ratio was measured in order to confirm that Kupffer cell depletion primarily affected liver accumulation, while the pegylation strategy caused a reduction in the accumulation of liposomes in other organs. The results indicate the pegylation increases the plasma/spleen accumulation ratio from 0.01 to 8.57, while the ratio increase was substantially less for Kupffer cell depletion (0.09) (Fig. 6c). Notably, PEG-shielding and Kupffer cell depletion did not completely eliminate liver deposition of liposomes, suggesting that other factors in addition to cell-mediated uptake play a role in organotropic accumulation of liposomes in the liver.

4. Conclusion

The results from this study suggest that Kupffer cells may not be the sole contributing factor in cell-mediated accumulation of liposomes in the liver, since pegylation was a more effective strategy than Kupffer cell depletion for avoiding deposition in this organ. This observation is coherent with the findings of Tsoi *et al.,* who investigated cell populations responsible for liver accumulation of hard nanoparticles, including quantum dots, gold nanoparticles, and silica nanoparticles. The authors found that several different cell types internalize nanoparticles in the liver [7]. In particular, Kupffer cells and hepatic B cells accounted for the largest contribution to nanoparticle uptake in this organ. Other cells such as hepatocytes and endothelial cells played a negligible role in liver accumulation of hard nanomaterials [7]. Notably, previous studies have not investigated the contribution of various cell types to the accumulation of soft nanoparticles in the liver, highlighting the need for further research on this topic.

It has previously been suggested that macrophage modulation approaches could be useful for improving nanodelivery [26]. Notably, Kupffer cell depletion has been associated with adverse events and deaths in mice studies [27], indicating that complete elimination of liver macrophages is unlikely to be a clinically viable strategy for improving the biodistribution of nanoparticles. Nevertheless, other less drastic approaches for modulating macrophage responses in the liver and spleen could be suitable for improving nanodelivery. However, it is questionable whether implementation of such strategies is necessary, since pegylation seems to be superior to Kupffer cell depletion. In this regard, it is important to consider that pegylation primarily delays nanoparticle uptake by the mononuclear phagocyte system rather than permanently blocking cell interactions. For instance, the stealth effect can gradually decrease due to the detachment of PEG-phospholipids from the lipid membrane [28, 29]. Therefore, macrophage modulation strategies are likely to be useful for reducing the clearance of pegylated nanoparticles after longer time periods. There are also several instances where the use of pegylated nanoparticles is undesirable, necessitating the implementation of alternative methods for reducing uptake by the mononuclear phagocyte system. For instance, repeated injections of pegylated nanoparticles can trigger the accelerated blood clearance (ABC) phenomenon, which causes rapid elimination of nanoparticles from the circulation as a result of antibody-mediated clearance [30]. Moreover, PEG has in some cases been found to activate the complement system [31, 32], which can result in accelerated clearance and adverse immune reactions [12, 33]. Nanoparticle pegylation is also associated with the PEG dilemma, which entails that the stealth effect pertains to all types of tissues [34]. Namely, although pegylation decreases nanoparticle

uptake by the mononuclear phagocyte system, it also reduces nanoparticle interactions with e.g. cancer cells. Therefore, in addition to stealth shielding of nanoparticles, there is a need to develop strategies for microenvironmental priming of the mononuclear phagocyte system.

Acknowledgments

This work was made possible with funds provided by the Houston Methodist Research Institute. Partial funds were acquired from: the US Department of Defense (W81XWH-09-1-0212, W81XWH-12-1-0414) (M.F.), the National Institutes of Health (U54CA143837, U54CA151668, U54CA210181) (M.F.), the Ernest Cockrell Jr. Distinguished Endowed Chair (M.F.), Victoriastiftelsen Finland (J.W.), Nylands nation Finland (J.W.), and the Cancer Prevention Research Institute 365 of Texas (RP121071) (M.F. and H.S.).

References

1. Wicki A, Witzigmann D, Balasubramanian V, Huwyler J. Nanomedicine in cancer therapy: Challenges, opportunities, and clinical applications. J Control Release. 2015; 200:138–157. [PubMed: 25545217]
2. Shen YA, Shyu L, Lu M, He CL, Hsu YM, Liang HF, Liu CP, Liu RS, Shen BJ, Wei YH. Bypassing the EPR effect with a nanomedicine harboring a sustained-release function allows better tumor control. Int J Nanomedicine. 2015; 10:2485. [PubMed: 25848266]
3. Suzuki R, Takizawa T, Kuwata Y, Mutoh M, Ishiguro N, Utoguchi N, Shinohara A, Eriguchi M, Yanagie H, Maruyama K. Effective anti-tumor activity of oxaliplatin encapsulated in transferrin–PEG-liposome. Int J Pharm. 2008; 346:143–150. [PubMed: 17640835]
4. Chau Y, Dang NM, Tan FE, Langer R. Investigation of targeting mechanism of new dextran-peptide-methotrexate conjugates using biodistribution study in matrix-metalloproteinase-overexpressing tumor xenograft model. J Pharm Sci. 2006; 95:542–551. [PubMed: 16419048]
5. Wilhelm S, Tavares AJ, Dai Q, Ohta S, Audet J, Dvorak HF, Chan WCW. Analysis of nanoparticle delivery to tumours. Nature Nat Rev Mater. 2016; 1:16014.
6. Gustafson HH, Holt-Casper D, Grainger DW, Ghandehari H. Nanoparticle uptake: The phagocyte problem. Nano today. 2015; 10:487–510. [PubMed: 26640510]
7. Tsoi KM, MacParland SA, Ma XZ, Spetzler VN, Echeverri J, Ouyang B, Fadel SM, Sykes EA, Goldaracena N, Kaths JM, Conneely JB, Alman BA, Selzner M, Ostrowski MA, Adeyi OA, Zilman A, McGilvray ID, Chan WC. Mechanism of hard-nanomaterial clearance by the liver. Nat Mater. 2016; 15:1212–1221. [PubMed: 27525571]
8. MacPhee PJ, Schmidt EE, Groom AC. Intermittence of blood flow in liver sinusoids, studied by high-resolution in vivo microscopy. Am J Physiol Gastrointest Liver Physiol. 1995; 269:G692–G698.
9. Menger MD, Marzi I, Messmer K. In vivo fluorescence microscopy for quantitative analysis of the hepatic microcirculation in hamsters and rats. Eur Surg Res. 1991; 23:158–169. [PubMed: 1782961]
10. Davies LC, Jenkins SJ, Allen JE, Taylor PR. Tissue-resident macrophages. Nat Immunol. 2013; 14:986–995. [PubMed: 24048120]
11. Bertrand N, Leroux JC. The journey of a drug-carrier in the body: an anatomo-physiological perspective. J Control Release. 2012; 161:152–163. [PubMed: 22001607]
12. Moghimi SM, Simberg D. Complement activation turnover on surfaces of nanoparticles. Nano Today. 2017
13. Pasut G, Veronese FM. State of the art in PEGylation: The great versatility achieved after forty years of research. J Control Release. 2012; 161:461–472. [PubMed: 22094104]
14. Walkey CD, Chan WC. Understanding and controlling the interaction of nanomaterials with proteins in a physiological environment. Chem Soc Rev. 2012; 41:2780–2799. [PubMed: 22086677]
15. Gregoriadis G, Swain C, Wills E, Tavill A. Drug-carrier potential of liposomes in cancer chemotherapy. The Lancet. 1974; 303:1313–1316.
16. Sercombe L, Veerati T, Moheimani F, Wu SY, Sood AK, Hua S. Advances and challenges of liposome assisted drug delivery. Front Pharmacol. 2015; 6:286. [PubMed: 26648870]

17. Chang HI, Yeh MK. Clinical development of liposome-based drugs: formulation, characterization, and therapeutic efficacy. Int J Nanomedicine. 2012; 7
18. Wolfram J, Scott B, Boom K, Shen J, Borsoi C, Suri K, Grande R, Fresta M, Celia C, Zhao Y. Hesperetin liposomes for cancer therapy. Curr Drug Deliv. 2015
19. Wolfram J, Suri K, Huang Y, Molinaro R, Borsoi C, Scott B, Boom K, Paolino D, Fresta M, Wang J. Evaluation of anticancer activity of celastrol liposomes in prostate cancer cells. J Microencapsul. 2014; 31:501–507. [PubMed: 24654943]
20. Scott B, Shen J, Nizzero S, Boom K, Persano S, Mi Y, Liu X, Zhao Y, Blanco E, Shen H. A pyruvate decarboxylase-mediated therapeutic strategy for mimicking yeast metabolism in cancer cells. Pharmacol Res. 2016; 111:413–421. [PubMed: 27394167]
21. Naito M, Nagai H, Kawano S, Umezu H, Zhu H, Moriyama H, Yamamoto T, Takatsuka H, Takei Y. Liposome-encapsulated dichloromethylene diphosphonate induces macrophage apoptosis in vivo and in vitro. J Leukoc Biol Suppl. 1996; 60:337–344.
22. Barenholz Y. Doxil(R)--the first FDA-approved nano-drug: lessons learned. Journal J Control Release. 2012; 160:117–134. [PubMed: 22484195]
23. Abraham SA, Waterhouse DN, Mayer LD, Cullis PR, Madden TD, Bally MB. The liposomal formulation of doxorubicin. Methods Enzymol. 2005; 391:71–97. [PubMed: 15721375]
24. Sadzuka Y, Nakade A, Hirama R, Miyagishima A, Nozawa Y, Hirota S, Sonobe T. Effects of mixed polyethyleneglycol modification on fixed aqueous layer thickness and antitumor activity of doxorubicin containing liposome. Int J Pharm. 2002; 238:171–180. [PubMed: 11996821]
25. Van Rooijen N, Sanders A. Liposome mediated depletion of macrophages: mechanism of action, preparation of liposomes and applications. J Immunol Methods. 1994; 174:83–93. [PubMed: 8083541]
26. Khalid A, Persano S, Shen H, Zhao Y, Blanco E, Ferrari M, Wolfram J. Strategies for improving drug delivery: nanocarriers and microenvironmental priming. Expert Opin Drug Deliv. 2016:1–13.
27. Li Z, Xu X, Feng X, Murphy PM. The Macrophage-depleting Agent Clodronate Promotes Durable Hematopoietic Chimerism and Donor-specific Skin Allograft Tolerance in Mice. Sci Rep. 2016; 6
28. Parr MJ, Ansell SM, Choi LS, Cullis PR. Factors influencing the retention and chemical stability of poly (ethylene glycol)-lipid conjugates incorporated into large unilamellar vesicles. Biochim Biophys Acta. 1994; 1195:21–30. [PubMed: 7918562]
29. Pasut G, Paolino D, Celia C, Mero A, Joseph AS, Wolfram J, Cosco D, Schiavon O, Shen H, Fresta M. Polyethylene glycol (PEG)-dendron phospholipids as innovative constructs for the preparation of super stealth liposomes for anticancer therapy. J Control Release. 2015; 199:106–113. [PubMed: 25499917]
30. Knop K, Hoogenboom R, Fischer D, Schubert US. Poly(ethylene glycol) in drug delivery: pros and cons as well as potential alternatives. Angew Chem Int Ed Engl. 2010; 49:6288–6308. [PubMed: 20648499]
31. Hamad I, Hunter AC, Szebeni J, Moghimi SM. Poly(ethylene glycol)s generate complement activation products in human serum through increased alternative pathway turnover and a MASP-2-dependent process. Mol Immunol. 2008; 46:225–232. [PubMed: 18849076]
32. Moghimi SM, Andersen AJ, Hashemi SH, Lettiero B, Ahmadvand D, Hunter A, Andresen TL, Hamad I, Szebeni J. Complement activation cascade triggered by PEG–PL engineered nanomedicines and carbon nanotubes: The challenges ahead. J Control Release. 2010; 146:175–181. [PubMed: 20388529]
33. Yang Q, Lai SK. Anti-PEG immunity: emergence, characteristics, and unaddressed questions. Wiley Interdiscip Rev Nanomed Nanobiotechnol. 2015; 7:655–677. [PubMed: 25707913]
34. Hatakeyama H, Akita H, Harashima H. The polyethyleneglycol dilemma: advantage and disadvantage of PEGylation of liposomes for systemic genes and nucleic acids delivery to tumors. Biol Pharm Bull. 2013; 36:892–899. [PubMed: 23727912]

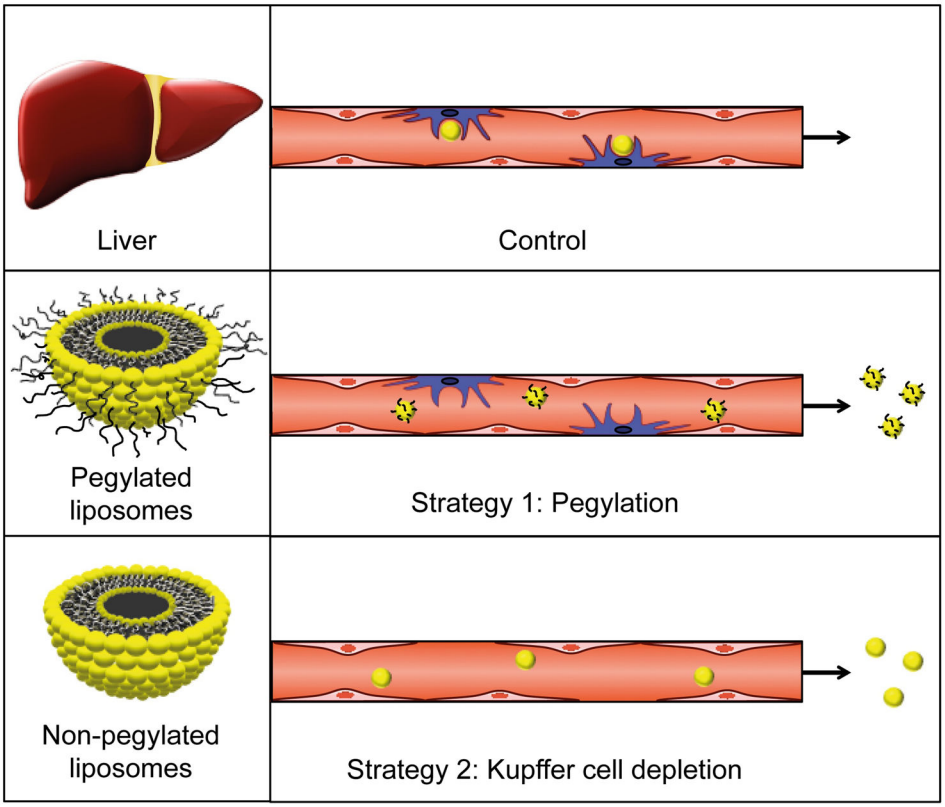

Figure 1.
Schematic representation of the two strategies used for reducing nanoparticle uptake in the mononuclear phagocyte system. In the control group, liposomes are taken up by Kupffer cells in the liver, while pegylation and Kupffer cell depletion decrease liposome accumulation in this organ.

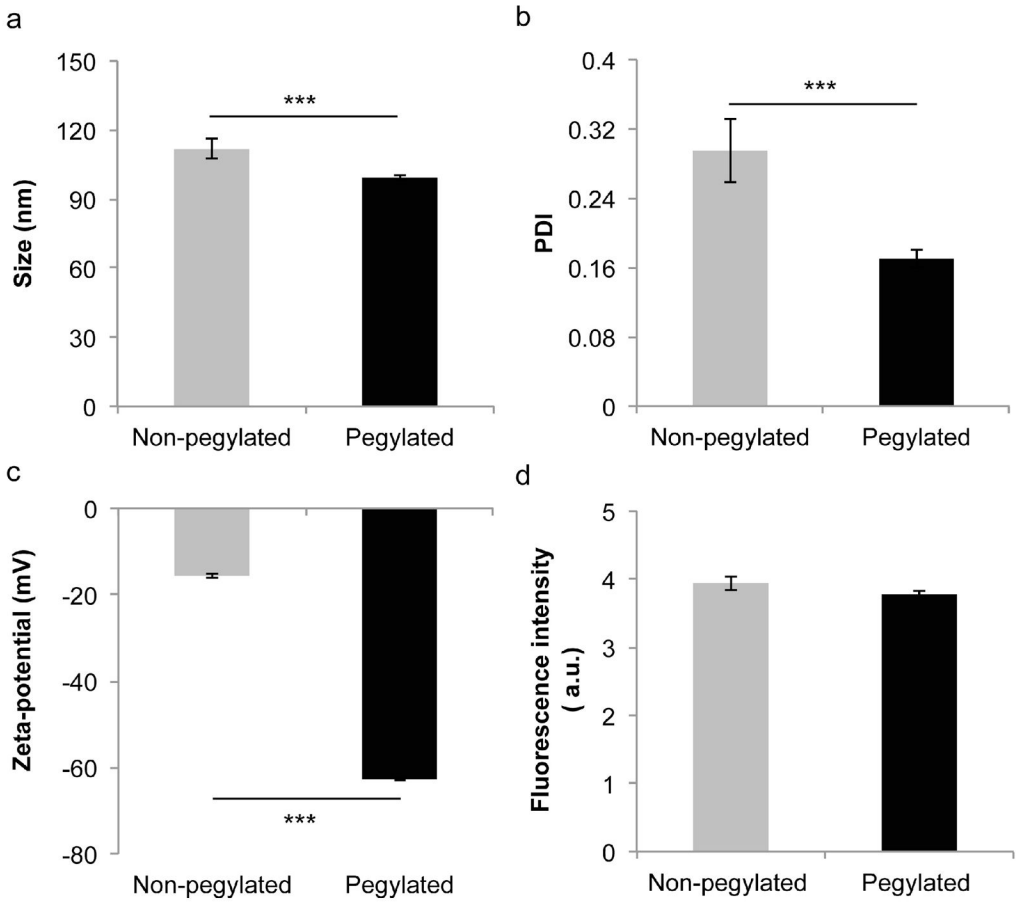

Figure 2.

Characterization of non-pegylated and pegylated liposomes. a) Size. b) PDI. c) Zeta potential. d) Fluorescence intensity. Results are expressed as the mean ± s.d. of five measurements with ten runs each (a, b, c) or triplicates (d). The student's t-test was used to calculate statistical significance. ***, $P < 0.001$. A.u., arbitrary unit.

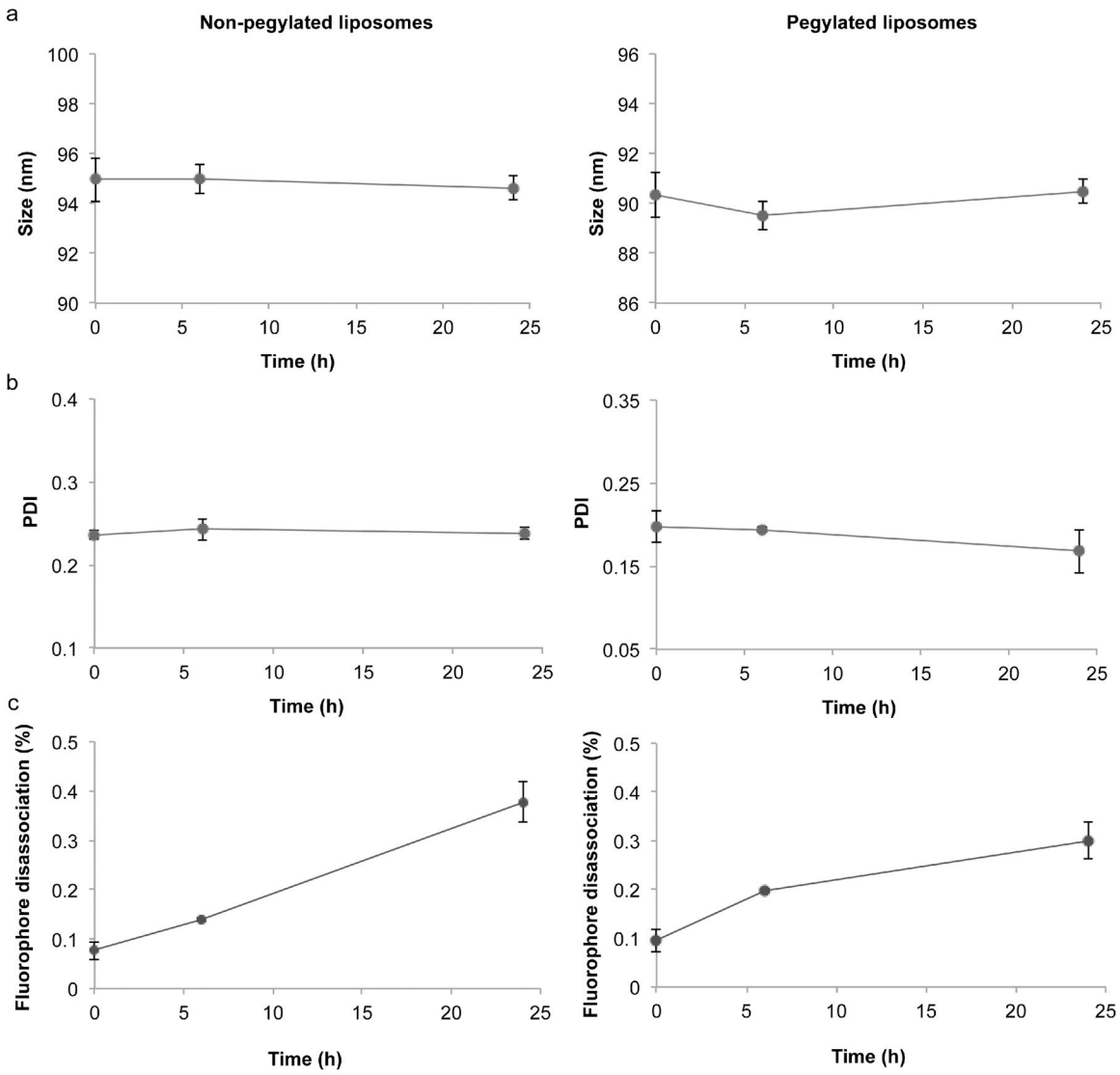

Figure 3.

Stability of pegylated and non-pegylated liposomes under physiological conditions. Liposomes were incubated with media containing fetal bovine serum at 37 °C with continuous shaking. The size (a), polydispersity index (PDI) (b), and fluorophore release (c) were measured periodically. Results are expressed as the mean ± s.d. of five measurements with ten runs each.

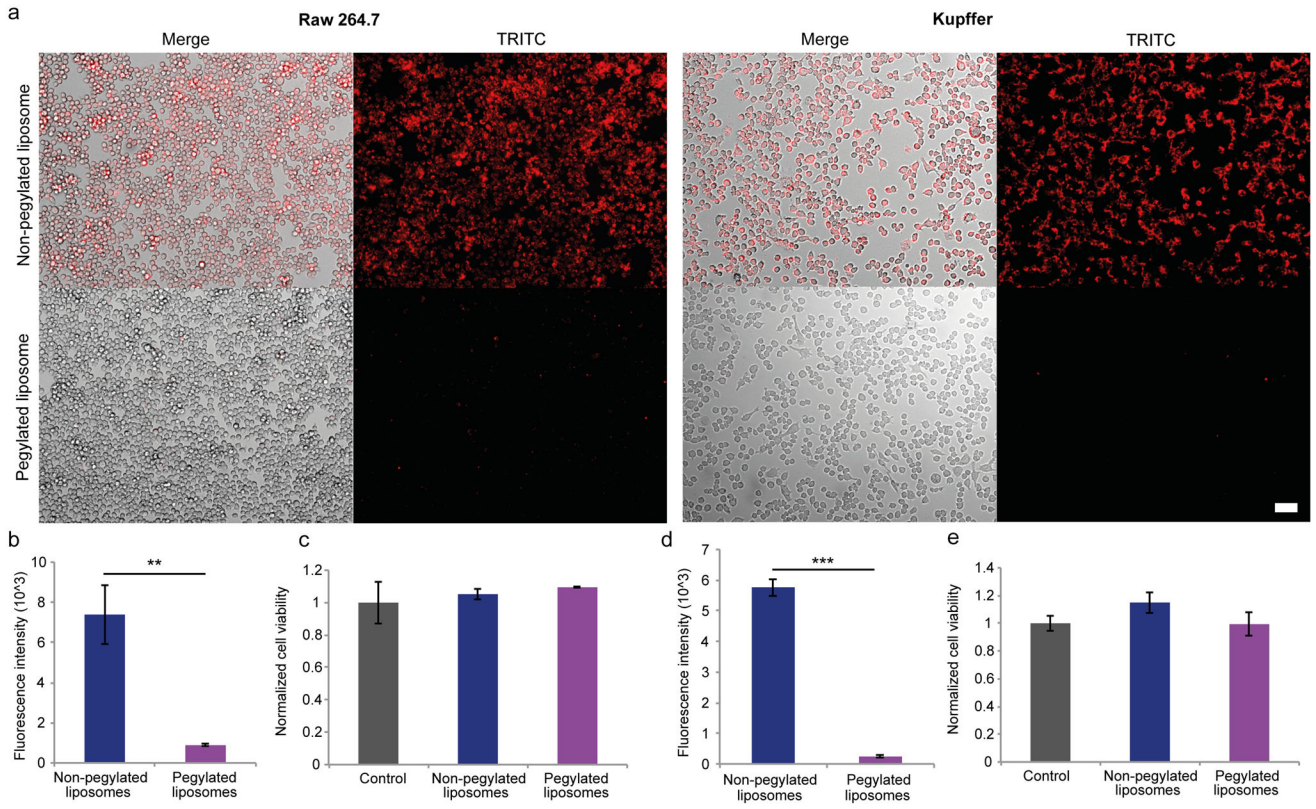

Figure 4.

Liposomal uptake and cell viability of macrophages. Fluorescently-labled non-pegyalated and pegylated liposomes were incubated for 3 h with Raw 264.7 cells and Kupffer cells. a) Representative images of liposome uptake. Scale bar, 50 μm. Quantitative measurements of fluorescence intensity of Raw 264.7 (b) and Kupffer (d) cells exposed to liposomes. Viability of Raw 264.7 (c) and Kupffer (e) cells exposed to liposomes. Results were normalized to the control cells. Data is presented as mean ± s.d. of triplicates. The Student's t-test was used to calculate statistical significance. **, $P < 0.01$; ***, $P < 0.001$.

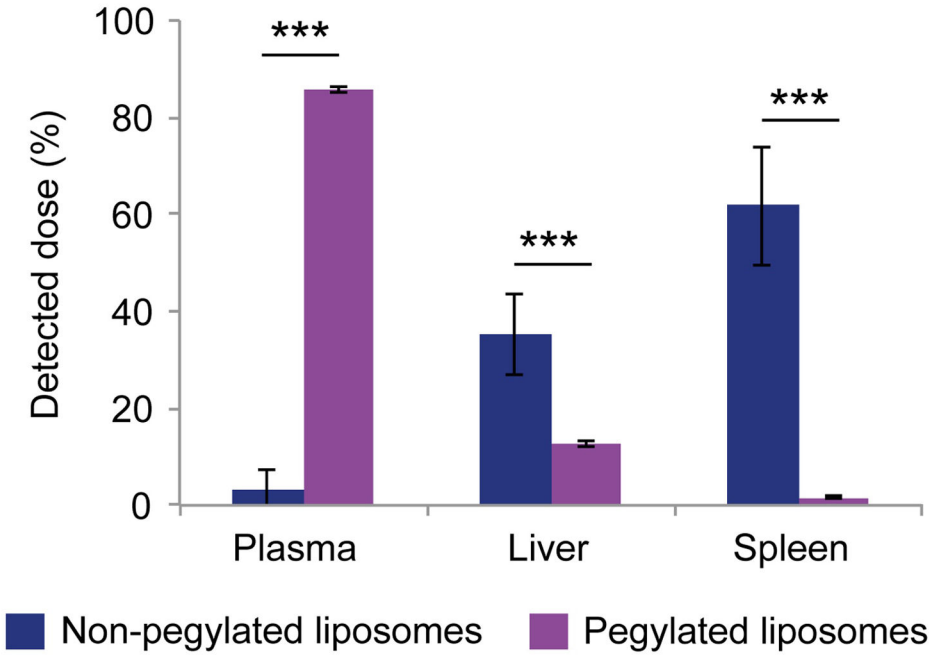

Figure 5.

Biodistribution of fluorescent non-pegylated and pegylated liposomes in mice. The plasma, liver, and spleen were collected 24 h after intravenous administration of liposomes. Data is presented as mean ± s.d. ($n = 5$). The student's t-test was used to calculate statistical significance. ***, $P < 0.001$.

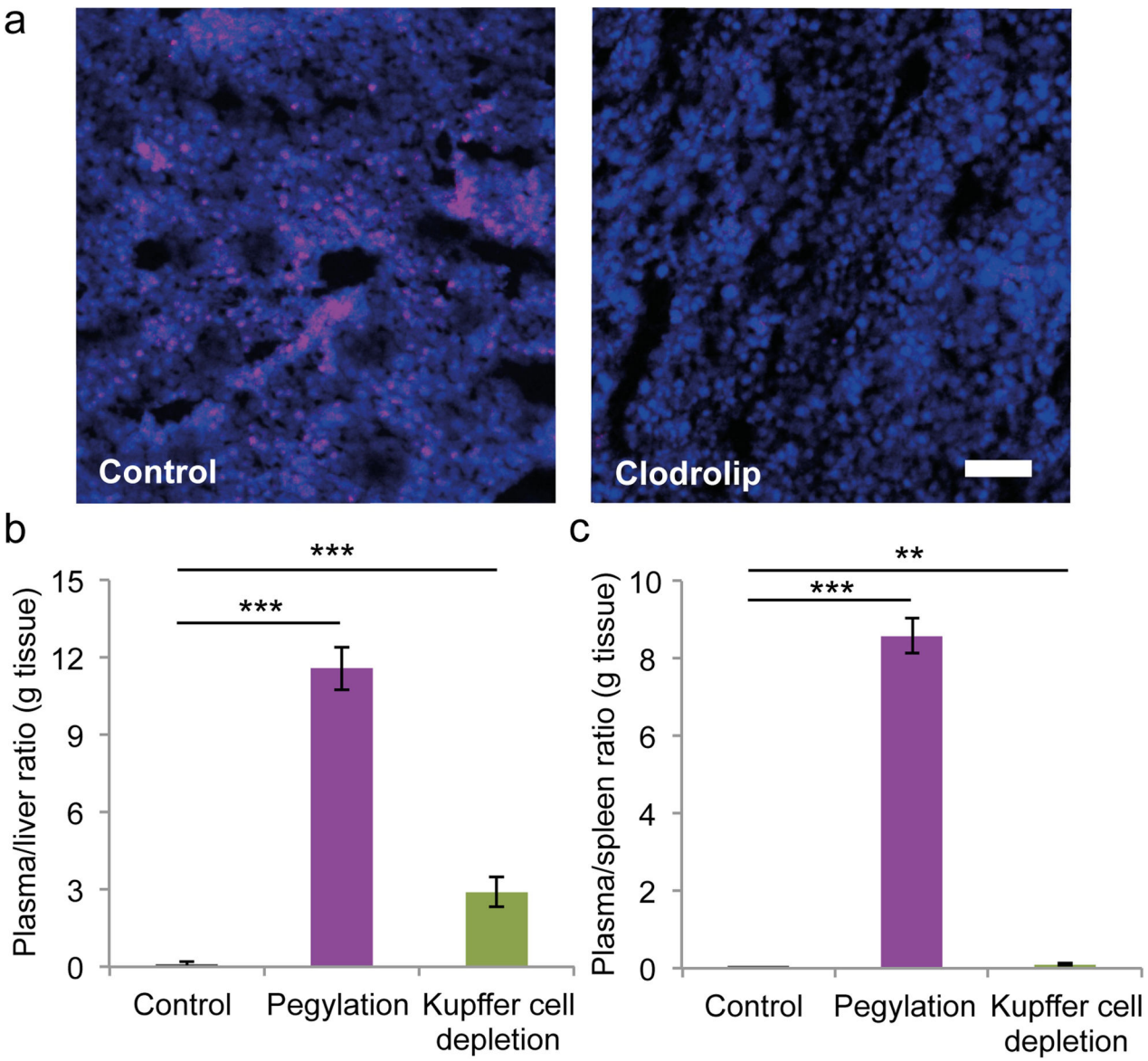

Figure 6.

Effect of pegylation and kupffer cell depletion on liposome accumulation in the mononuclear phagocyte system of mice. (a) Immunofluorescence images of liver sections. Kupffer cell depletion was achieved with intravenous injections of clodronate liposomes (clodrolip; 50 mg/kg clodronate). Kupffer cells, purple (F4/80 antibody); DAPI, blue. Scale bar, 100 μm. (b,c) The plasma/liver (b) and plasma/spleen (c) liposome accumulation ratios (g tissue) 24 h after intravenous injection. Data is presented as mean ± s.d. ($n = 5$). The student's t-test was used to calculate statistical significance. **, $P < 0.01$; ***, $P < 0.001$.